Abstract—Sagittal otoliths (*n*=208) were removed from larval Gulf menhaden (*Brevoortia patronus*) collected in a Louisiana tidal pass over a 2-year period, from October 2006 to March 2007 and from September 2007 to March 2008, and analyzed with digital imaging and fast Fourier transformations to estimate age and growth. Length at age was estimated by using a 2-cycle Laird–Gompertz growth model and the growth rates were found to be relatively consistent with rates from previous research in the northern Gulf of Mexico, and the estimated timing of an ontogenetic shift in feeding strategy occurred at approximately 33 days after spawning. Laird–Gompertz growth models fitted separately to age and length groupings revealed that the ontogenetic shift was correlated more with larval age than with length. Measurements taken from digital images were used to conduct fine-scale analyses of otolith microstructure and confirmed that a change in otolith structure coincided with the ontogenetic shift in feeding at approximately 33 days after spawning. Keys of length frequencies at age were used to assess temporal variability in Gulf menhaden spawning and they revealed earlier (i.e., September) recruitment to spawning and estuarine areas and shorter recruitment corridors than those previously reported.

Effects of recruitment through a coastal hydrodynamic boundary layer on growth and otolith microstructure of larval Gulf menhaden (*Brevoortia patronus*)

Matthew J. Kupchik (contact author)[1]
Richard F. Shaw[2]

Email for contact author: mkupch1@lsu.edu

[1] Department of Oceanography and Coastal Sciences
College of the Coast and Environment
Louisiana State University
2143 Energy, Coast, and Environment Building
Baton Rouge, Louisiana 70803

[2] Department of Oceanography and Coastal Sciences
College of the Coast and Environment
Louisiana State University
1002Q Energy, Coast, and Environment Building
Baton Rouge, Louisiana 70803

The Gulf menhaden (*Brevoortia patronus*) is both the target of a commercially important fishery in the Gulf of Mexico (GOM; Pritchard, 2005; Vaughan et al.[1]; McCrea-Strub et al., 2011) and is an ecologically important prey item for commercially and recreationally valuable species (Del Rio et al., 2010; Nelson et al., 2012; Simonsen and Cowan, 2013). Gulf menhaden have an established distributional range from the western central Atlantic to the GOM, and specifically within the GOM from Florida Bay to the Bay of Campeche (Whitehead, 1985). The Gulf menhaden fishery is the second largest United States fishery by both weight and value (Pritchard, 2005), and this reduction fishery harvests an average of 400–600 kilotons annually. In recent years, 92% of the annual landings occurred in Louisiana (Vaughan et al.[1]). There is also a second, and minor component of annual landings collected by the small bait fishery in the GOM (VanderKooy and Smith[2]). Although the stock is relatively healthy with a lower fishing-induced mortality rate than that reported for target fishing over the long term, in recent years fishing mortality has increased above the target level, but below the mortality limit, and population fecundity has decreased (Vaughan et al., 2007). Possible limitations to population growth for Gulf menhaden include food availability, habitat limitations, and successful recruitment of larvae into estuarine nursery areas, but with declining recruitment being more of a concern

[1] Vaughan, D. S., J. W. Smith, and A. M. Schueller. 2010. Age, growth and reproduction of gulf menhaden. Southeast Data, Assessment, and Review SEDAR 27-DW02, 34 p. [Available from website.]

[2] VanderKooy, S. J., and J. W. Smith (eds.). 2015. The menhaden fishery of the Gulf of Mexico, United States: a regional management plan, 2015 Revision, 201 p. Gulf States Mar. Fish. Comm., Ocean Springs, MS. [Available from website.]

on the basis of a decrease in population fecundity over the last decade (Vaughan et al., 2007).

Gulf menhaden are estuarine dependent and reportedly spawn from October through February (Whitehead, 1985; Nelson and Ahrenholz, 1986; Vaughan et al., 2000) and the peak estuarine recruitment occurs in late January and early February (Lewis and Roithmayr, 1981; Shaw et al., 1988). Spawning depth for Gulf menhaden is usually 90 m and shallower (Whitehead, 1985; Powell, 1994), and spawning locations occur farther offshore as the season progresses, suggesting shorter "recruitment corridors" (Cushing, 1975) during fall recruitment (Vaughan et al., 2007). Mean egg diameter has been reported to be 1.61 mm, and length at hatching to be approximately 3 mm total length (Dahlberg, 1970; Lewis and Roithmayr, 1981; Shaw et al., 1985). The pelagic eggs take 2–3 days to hatch and another 2–3 days until yolk absorption is complete, with the result that first feeding and first otolith increment formation occur approximately 5 days after spawning (Warlen, 1988). Offshore larval drift and cross shelf transport have been reported to take between 4 and 10 weeks (Shaw et al., 1988). The variability in transport times is tied to the limited swimming capacity of larval fish (Shanks and Eckert, 2005); successful estuarine recruitment is therefore driven more by oceanographic flows (Guillory et al., 1983; Epifanio and Garvine, 2001; Gillanders et al., 2003). Recruitment from more oligotrophic inner continental shelf spawning grounds through the hydrodynamically variable oceanographic coastal boundary layer, which is produced by atmospheric effects, into tidal passes, and ultimately more productive estuarine waters (Raynie and Shaw, 1994) corresponds with the time period when Atlantic menhaden (*Brevoortia tyrannus*) and Gulf menhaden larvae transform from selective particulate feeding to omnivorous filter-feeding juveniles (Stoecker and Govoni, 1984; Deegan, 1990; Chen et al., 1992; Lozano et al., 2012). This transformation begins at approximately 20 mm standard length (SL) and is completed by approximately 30 mm SL (Hettler, 1981; Warlen, 1988), with a corresponding increase in gill raker counts. For example, gill raker counts were recorded to increase from 5 +14 to 13 +25 for larvae between 19 and 22 mm SL, as they were beginning to undergo metamorphosis in Lake Pontchartrain, Louisiana (Suttkus, 1956).

Studies of larval Gulf menhaden age and growth in Louisiana have focused on both the offshore (Shaw et al., 1985, 1988; Warlen, 1988; Raynie and Shaw, 1994) and inshore components of the recruitment corridor (Deegan and Thompson, 1987; Marotz et al. 1990; Raynie and Shaw, 1994). These studies have reported growth rates between 0.28 and 0.42 mm/day for the smaller larvae typically encountered on the continental shelf (Deegan and Thompson, 1987; Raynie and Shaw, 1994) and between 0.11 and 0.12 mm/day for larvae collected within Sabine Pass and Fourleague Bay, Louisiana (Warlen, 1988; Raynie, 1991).

Daily growth increments in otoliths have been confirmed in larval Gulf menhaden in laboratory studies (Warlen, 1988). The daily rings in otoliths of larval fish can provide growth rates and can act as a proxy for identification of changes in developmental stages and for environmental stress reflected in the variability in otolith ring width (Maillet and Checkley, 1990, 1991; Chambers and Miller, 1995). Analysis of larval otolith structure was initially done by visual inspection; however, video and digital methods have become prevalent with an increase in computing resolution and digital imaging (Ralston and Williams, 1989; Campana, 1992; Morales-Nin et al., 1998). Regardless of what ring counting method is being used, the ring structure must be verified because the shape and relative size of otoliths are species specific and genetically controlled (Schmidt, 1969; Gaemers, 1976; Nolf, 1985; Lombarte and Morales-Nin, 1995; Morales-Nin et al., 1998).

The objectives of our study were as follows. First, to determine the length at age of Gulf menhaden for the sampling period. Second, to determine at what age there is a shift in growth rate consistent with the expected shift in feeding strategy from a selective particulate feeder to an omnivorous filter feeder. Third, to compare otolith microstructure with length at age models for confirmation of growth rate and shift in feeding strategy upon entering the coastal boundary layer and the transition from oceanic to estuarine waters. Fourth, to determine the distribution of the spawning period by using back calculation of spawning dates from age frequency keys. Fifth, to determine the duration of the recruitment corridor from offshore spawning grounds across the coastal boundary layer, and into the estuarine nursery grounds.

Materials and methods

Sampling location

Samples of ichthyoplankton were collected near the Port of Fourchon, in Bayou Tartellan, Louisiana (Fig. 1). This sampling location is connected to the GOM at Belle Pass (29°5′53.9″N, 90°13′17.8″W) and is one of the first major inland bifurcations of the tidal pass. The tidal pass and Bayou Tartellan are seasonally well mixed and have limited temperature, salinity, or dissolved oxygen stratification. Bayou Tartellan is also characterized by high turbidity, and a low volume of freshwater input owing to a limited drainage basin. The sampling location (29°6′49″N, 90°11′4″W) was determined to maximize flow rates for passive sampling of the tidal pass. The passive sampling was conducted from the end of a 3.7-m-long dock on the northern bank of the tidal pass, which had a sampling depth of 10 m and an overall tidal pass width of approximately 73 m.

Field methods

Individual samples of ichthyoplankton were collected passively with a 60-cm ring net (with 333-µm mesh, and 2 m in length) that was dyed dark green to mini-
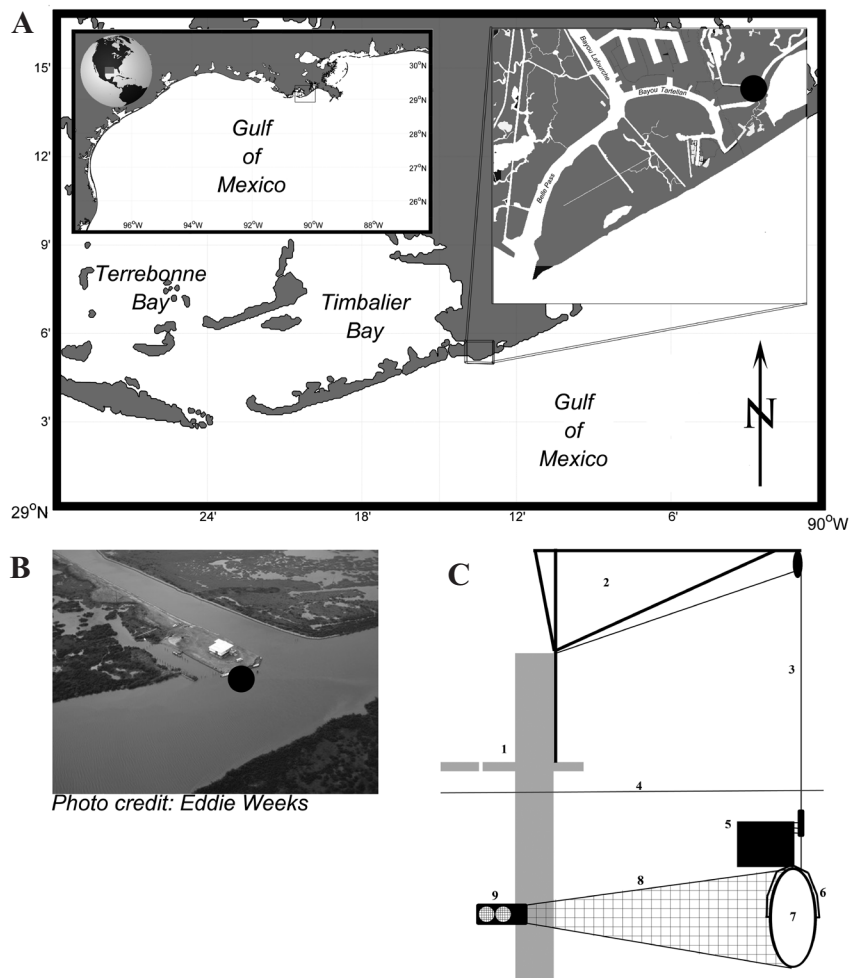
Figure 1

(**A**) Map of the sampling location for this study in relation to the Gulf of Mexico and coastal Louisiana. The upper right inset represents the area around Port Fourchon, Belle Pass, Louisiana, and the sampling site in Bayou Tartellan identified by a black circle on the map. Sampling for larval Gulf menhaden (*Brevoortia patronus*) was conducted from October 2006 through April 2007 and again from September 2007 through April 2008. (**B**) Aerial photograph of the sampling site at Bayou Tartellan; the black circle again identifies the sampling site. (**C**) Diagram of the sampling system: 1) fixed dock where the sampling system was attached, 2) davit that was used to extend the net farther into the channel, 3) cable system by which the net was raised and lowered, 4) water surface, 5) orientation vane for the net system, 6) 60-cm metal ring that held open the net mouth, 7) pivoting gimbal, 8) 333-µm mesh net, dyed dark green, and 9) plastic, vinyl-coated codend with 333-µm drainage ports.

mize avoidance of the net. The ring net was outfitted with a gimbal and current vain for proper net orientation. The net system was raised and lowered for sampling and collection of samples by using a fixed davit, from which was suspended a stainless steel cable from above the sampling deck to the channel bottom. Samples were collected by using a plastic vinyl coated codend with 333-µm-mesh drainage ports attached to the end of the net. To determine the volume of filtered water, a flowmeter (model no. 2030; General Oceanics

Inc.[3], Miami, FL) was positioned slightly off center of the ring to determine the volume of water filtered.

Samples were collected every 4 h over a 72-h period, twice monthly between the months of October and April, over a 2-year period (2006–2008), except during December and January, which were sampled

only monthly. In addition, 2 sampling efforts occurred in September 2007. The sampling design was developed to focus on atmospheric cold front passages, which are intermittent wind-dominated meteorological events common from the late fall through early spring along the Louisiana coast. Individual sampling dates were chosen to maximize sampling during astronomical tidal ranges to better evaluate the potential impacts of these atmospheric events. Ichthyoplankton were collected randomly and passively from both the surface and near-bottom. Collections at the surface were 6 min in duration, and net samples collected near-bottom were 10 minutes. These differences in sampling duration were chosen to attempt to have similar volumes of water filtered through the net. To prevent contamination of the net during deployment for near-bottom sampling, the net mouth was closed until the ring net was at depth, and was closed again after sampling for retrieval. Nets were rinsed and washed down with fresh water to avoid sample contamination. All ichthyoplankton sampling was conducted under pre-approved planning and authorization by the Institutional Animal Care and Use Committee.

Ichthyoplankton samples were initially preserved in 10% buffered (sodium phosphate, dibasic $NaH_2PO_4 \cdot H_2O$ and monobasic Na_2HPO_4) formalin—a short-exposure, long-term fixative—for approximately 3.5 h. Samples were then rinsed and transferred to a 70% ethanol solution for long-term storage and for later examination of the larval fish otoliths.

Estuarine hydrographic parameters were measured at dockside during each plankton sampling event by using a portable YSI Model 85 instrument (YSI Inc., Yellow Springs, CO) to collect data on temperature, conductivity (salinity), and dissolved oxygen at each depth during net deployment. Data concerning predicted diurnal tides, measured tide height, and the resulting alteration in the expected tidal prism were collected from a nearby tide gauge station (station ID: 8762075; NOAA Tides and Currents, website) at the Port of Fourchon, Belle Pass, Louisiana (29°6.8′N, 90°11.9′W).

Laboratory methods

A Motodo Plankton Splitter (Aquatic Research Instruments, Hope, ID) was used to split samples with volumes greater than 200 mL in half and to split samples with a volume greater than 400 mL into quarters. All ichthyoplankton were removed from the samples and placed into 10-mL scintillation vials by using a dissecting stereoscope. To ensure that all ichthyoplankton were removed, a random subset of samples from both surface and near-bottom collections were checked by a second party after initial processing.

Ichthyoplankton were identified to the lowest taxonomic classification possible; however, size and physical condition were potentially limiting factors for definitive confirmation of identification. Alizarin blue and alizarin red were used to confirm meristic counts for indi-

vidual ichthyoplankton that were difficult to identify. Gulf menhaden larvae were separated and stored in 70% ethanol for otolith analysis. Identifications of larval fish were based on identification guides by Richards (2005) and Fahay (2007).

Gulf menhaden were subsampled from each surface and near-bottom sample for otolith analysis on the basis of the normal distribution of SL of all Gulf menhaden larvae collected. Measurements of SL to the nearest 0.1 mm were taken with a Leica MZ6 stereoscope (Leica Microsystems, Buffalo Grove, IL) calibrated against a microscope stage micrometer. Gulf menhaden larvae were subsampled from every sampling effort that contained the target species. In samples where 3 or fewer Gulf menhaden larvae were collected, all larvae were selected for otolith removal. In samples that contained more than 3 Gulf menhaden larvae, 3 larvae were selected so that a larva with the longest SL, shortest SL, and a SL from the normal distribution was chosen for otolith removal. Removal, preparation, analysis and otolith interpretation were undertaken according to the methods described in Kupchik and Shaw (2016).

Age determination and spawning dates

Age of larval gulf menhaden, recorded in days after spawning (das), was determined from the counts of growth increments (otolith radii) by using a semi-automated image analysis method (Kupchik and Shaw, 2016). Daily increment deposition has been confirmed to have an increment-count to age-regression slope of 1 for larval Gulf menhaden growth (Geffen, 1992). As with the method used by Raynie (1991), we applied a 5-day lag for the first increment formation after spawning for Gulf menhaden larvae on the basis of laboratory research (Warlen, 1988). This lag resulted in a calculation of total age das where 5 days were added to the number of increments from read otoliths. For modeling growth, we applied a 3-day lag for first increment formation after hatching (Warlen, 1988). This resulted in a calculation in total age in days after hatching (dah) where 3 days are added to the number of increments determined from otolith reading. Ages were estimated for larvae not selected for dissection by using frequency of age-at-length keys and the FSA package, vers. 0.7.4, for R software, vers. 3.1.1 (R Core Team, 2014).

Spawning dates were calculated for all Gulf menhaden larvae; direct calculation was made for those larvae where otolith radii were analyzed, and also for those where the age was estimated with the method described by Isermann and Knight (2005), namely with a semi-random method in the FSA package. The spawning date was determined as the difference between the date of capture and the age in days after spawning.

Growth rates

Distributions of lengths and calculated ages based on increment counts were tested for normality by using a Shapiro–Wilk's test. Instantaneous larval growth (per

day) is expected to be fastest soon after first feeding, to decrease thereafter, and a large decrease or growth stanza is associated with an ontogenetic shift in feeding from selective particulate feeding to omnivorous filter feeding (Deegan, 1990; Lozano et al., 2012) in combination perhaps with transgressing the coastal boundary layer. To represent this shift in feeding strategy between the larval and juvenile stages, a derivative of the Gompertz model (Gompertz, 1825) was chosen because it highlights this specific pattern of growth. Larval somatic growth of Gulf menhaden was modeled by applying only the directly analyzed otolith data to a 2-cycle Laird–Gompertz growth model (Laird et al., 1965; Zweifel and Lasker, 1976; Raynie, 1991), and fitting the model with the use of R software. The 2-cycle Laird-Gompertz growth model is represented by the following equation:

$$L_t = L_{null} e^{[\frac{\gamma(1-e^{(-\alpha\Delta_1)})}{\alpha} + \frac{\delta(1-e^{(-\beta\Delta_1)})}{\beta}]}$$

$$\Delta_1 = MIN(t, t^*), \text{and}$$

$$\Delta_2 = MAX(t - t^*, 0), \qquad\qquad (1)$$

where L_t = the SL (in millimeters) at age (dah);
     L_{null} = SL at hatching for Gulf menhaden; and
        γ = $\frac{A}{\alpha}$
where A = the age specific instantaneous growth rate at spawning;
     α = the rate of exponential decay in growth rate before t^*;
    t^* = the time at which there is a shift between somatic growth stages;
     δ = $\frac{B}{\beta}$
where B = the age specific instantaneous growth rate immediately after the stage shift at $t = t^*$; and
     β = the exponential decay in growth in B.

The length at hatching was estimated but was based on literature. To increase model speed, length at hatching was constrained between 1 and 4 mm on the basis of the literature reporting between 2 and 4 mm (Hettler, 1981; Warlen, 1988; Powell, 1994; Raynie and Shaw, 1994). Similarly, t^* was estimated with a lower bound constraint of 20 dah, and an upper bound constraint of 45 dah (Suttkus, 1956; Hettler, 1981; Raynie, 1991). Hind-casting to estimate growth rates for larvae at ages not sampled, owing to larvae being offshore at these early ages, can be accomplished by using this 2-cycle Laird–Gompertz growth model (Lozano et al., 2012). The 2-cycle Laird–Gompertz model was applied to the pooled otolith data, and to each of the 2 sample years. Comparison between the yearly and pooled models was conducted with an F-test in R software.

The Laird parameterization of the Gompertz growth model was applied to both the pre-ontogenetic transformation period and the postontogenetic transformation period for groupings based on SL from the distribution of SLs of larvae whose otoliths were examined and based on the estimated transformation age from previous literature (Raynie, 1991). The Laird-Gompertz model was fitted by using R software and took the following form:

$$L_t = L_{null} e^{k(1-e^{-at})}, \qquad\qquad (2)$$

where L_t = the SL (in millimeters) at age t (days);
     L_{null} = SL at hatching for Gulf menhaden;
        a = the rate of exponential decay; and
        k = a dimensionless parameter so that ka represents the instantaneous growth rate at hatching.

Hind-casting can also be used to estimate growth rates for larvae at ages not sampled with this model structure (Lozano et al., 2012).

Changes in the magnitude of growth rate were measured by using differences in the width of the daily increments and variation in ring distance from the otolith core. Changes in otolith ring width and distance from the core are expected to occur after the ontogenetic shift in feeding strategy. Ring width was measured with the method described by Kupchik and Shaw (2016), and mean ring distance from the core and mean ring width were calculated for both the sampling period from October 2006 to March 2007 and the period from September 2007 to March 2008.
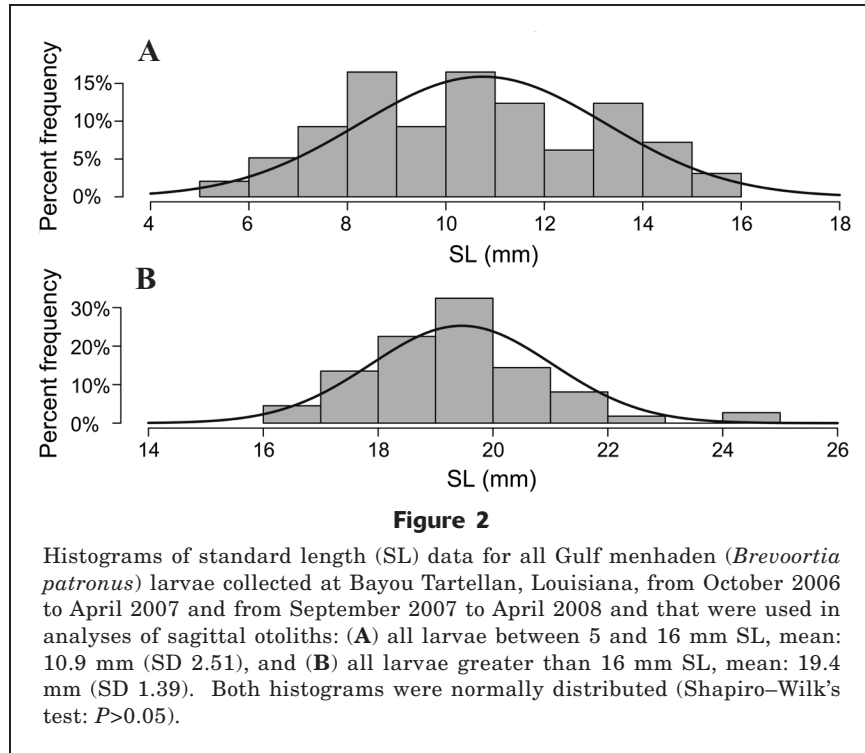
Results

Hydrology

Water temperatures based on sampling depth yielded no statistical differences—a result that is consistent with a seasonally, vertically well-mixed tidal pass. Water temperatures (mean: 20.5°C) generally had low variability during any sampling effort. However, from late November 2006 to early February 2007, recorded temperatures were colder and fluctuations were greater than those during other sampling efforts. In particular, the January 2007 sampling had a maximum difference of 10.2°C during the 72-h sampling period. Water temperatures were warmer during September and October, cooled from November through February, and then began to warm again in March and April. During November 2006, there was a large decrease in water temperature, and median water temperatures for each sampling effort remained below 15°C until early February 2007. In November 2007, there was also a decrease in water temperature; however, median water temperatures remained higher than 17°C for all subsequent sampling efforts.

Seasonality of larval Gulf menhaden collections

There were 2846 Gulf menhaden larvae collected in Bayou Tarellan during the sampling efforts from October 2006 to April 2008; 2158 larvae were collected during year 1, October 2006 to March 2007, and 688 larvae were collected during year 2, September 2007 to March

Figure 2

Histograms of standard length (SL) data for all Gulf menhaden (*Brevoortia patronus*) larvae collected at Bayou Tartellan, Louisiana, from October 2006 to April 2007 and from September 2007 to April 2008 and that were used in analyses of sagittal otoliths: (**A**) all larvae between 5 and 16 mm SL, mean: 10.9 mm (SD 2.51), and (**B**) all larvae greater than 16 mm SL, mean: 19.4 mm (SD 1.39). Both histograms were normally distributed (Shapiro–Wilk's test: *P*>0.05).

2008. January 2007 accounted for 40% of all larvae collected during the period from October 2006 to March 2007, and 30.3% of the total number of Gulf menhaden larvae were collected over both years. November 2007 collections had the second highest number of larvae, accounting for 26.3% of all Gulf menhaden larvae collected in year 2, and 6.4% of all larvae collected across both sampling years.

Length, age, and spawning dates

There were a total of 240 Gulf menhaden larvae that had sagittal otoliths removed for analysis. Thirty-two otoliths did not produce readable radii and were excluded from analysis. The length frequency of all larval Gulf menhaden that were aged (*n*=208) did not follow a normal distribution (Shapiro–Wilk: *P*<0.0001). As a result, we split the overall distribution into 2 groups to achieve 2 normal distributions, one of larvae between 5 and 16 mm SL (mean: 12.1 mm SL [standard deviation (SD) 3.71]) and the second consisting of larvae greater than 16 mm SL (mean: 19.4 mm SL [SD 1.39]; Fig. 2). The mean SL in year 1 was 14.7 mm (SD 4.61), and the mean SL for year 2 was 16.3 mm (SD 4.83), with a slightly larger range. Overall, the largest larvae were collected from January through March. In year 1 the largest larvae were collected in January 2007, in year 2 the largest larvae were collected in March 2008.

Combining both sample years, larval Gulf menhaden had a mean age of 32.3 das (SD 12.15), a median of 31.5 das, and a range of 11–67 das. For year 1, October 2006 to March 2007, the ages ranged from 15 to 67 das,

and a maximum density between 18 and 24 das. Also in year 1, the oldest larvae were collected in the largest numbers between December 2006 and February 2007. In year 2, September 2007 to March 2008, the highest densities were for larvae between 35 and 45 das, and the oldest larval Gulf menhaden were collected in March 2008.

In both sampling years, approximately half of all spawning dates for larvae sampled in Bayou Tartellan occurred before mid-January, and the other half occurred later in the year. In year 1, the greatest number of spawning dates occurred from 1 to 28 February 2007, and a smaller secondary peak occurred in October 2006 (Table 1). During year 2, the greatest number of spawning dates occurred between 16 January and 15 February 2008, and a second smaller peak occurred in late October or early November 2007.

Gulf menhaden growth rates

The 2-cycle Laird-Gompertz growth model provided a model fit that accounted for a faster initial growth rate and for a slower growth rate after the ontogenetic change (Fig. 3). The shift in growth rate and feeding pattern was estimated in the model to occur after 31 dah (*t**=31.086), or 33 das. The model estimated that length at hatching was 3.34 mm SL, and an age-specific growth rate at hatching of 0.0014/day. During this larval stage, the maximum growth rate was 0.72 mm/day, and mean growth rate was 0.47 mm/day. After the start of the developmental shift, at the modeled SL of 17.88 mm, the age-specific growth rate was 0.0006/day. The

Table 1

Spawning intervals for larval Gulf menhaden (*Brevoortia patronus*) collected in Bayou Tartellan, Louisiana, during 2006–2008. Spawning dates were determined from back-calculated otolith ages and collection dates after application of age–length keys. Percentages of the total number of larvae collected in each sampling year and cumulative percentages for each sampling year are based on half-month intervals.

Interval	2006–2007		2007–2008	
	%	Cumulative %	%	Cumulative %
09/01–09/15	0.07	0.07	0.20	0.20
09/16–09/30	1.39	1.46	0.40	0.61
10/01–10/15	15.28	16.74	1.97	2.58
10/16–10/31	8.45	25.19	9.91	12.49
11/01–11/15	2.95	28.14	10.12	22.61
11/16–11/30	2.49	30.63	4.86	27.47
12/01–12/15	6.79	37.42	11.33	38.80
12/16–12/31	9.70	47.12	8.50	47.29
01/01–01/15	2.49	49.62	5.92	53.21
01/16–01/31	6.58	56.20	14.67	67.88
02/01–02/15	20.96	77.17	19.47	87.35
02/16–02/28	19.13	96.29	7.28	94.64
03/01–03/15	2.25	98.54	3.95	98.58
03/16–03/31	1.46	100.00	1.42	100.00

initial portion of this growth stanza had a maximum growth rate of 0.21 mm/day, and an average growth rate of only 0.11 mm/day. The 2-cycle Laird–Gompertz models were also fitted separately to year 1 (October 2006 to March 2007) and year 2 (September 2007 to March 2008); however, these 2 models did not result in better performance over the pooled model (*F*-test: *P*=0.201; Fig. 3).

Individual Laird–Gompertz models were fitted for pre- and postmetamorphosis, first where the stages are delineated by age, and secondly where the stages are determined from SL. The breakdown by age between the 2 Laird–Gompertz models provided better fits in describing somatic growth during each period in contrast with the grouping determined by SL because of the increased variability in length at a particular age. The first Laird–Gompertz model for larval stage based on age groupings had an initial specific growth rate of 0.072/day, and a weaker decay rate of 0.019. This larval stage had a modeled maximum growth rate of 0.71 mm/day, and a mean growth rate of 0.47 mm/day (Fig. 4A). During the initial portion of the transition to the juvenile developmental stage, the decay rate for the age-grouped model was 0.051. This stage in the age-grouped model had a maximum growth rate of 0.20 mm/day, and an average growth rate of 0.08 mm/day. The premetamorphic larval stage for the SL grouping had an initial specific growth rate of 0.086/day, and a decay rate of 0.041. This premetamorphic stage had a modeled maximum growth rate of 0.41 mm/day, and

a mean growth rate of 0.38 mm/day (Fig. 4B). At the onset of metamorphosis to the juvenile developmental stage, the decay rate was 0.015. The very beginning of the ontogenetic shift to the juvenile developmental stage had a comparatively lower maximum growth rate of 0.12 mm/day, and an average growth rate of 0.10 mm/day.

Analyses of otolith microstructure showed changes in both mean ring distance from the otolith core, as well as in mean ring width after 33 das. Mean ring distance from the core during the initial larval stage was similar for both October 2006 to March 2007 and September 2007 to March 2008. After the beginning of the model-estimated ontogenetic shift at approximately 33 das, otolith growth slowed and showed limited variability, and year 2 otolith growth was slower than that of year 1 (Fig. 5A). Mean ring width showed a similar pattern: a decline in ring width occurred after 33 das and limited differences between either sampling years. Before the beginning of the ontogenetic shift onset, ring width for both sample years appeared to increase slightly, agreeing with the 2-cycle modeled growth rate that was largest just before the expected onset of shift in feeding strategy (Fig. 5B).

Discussion

Hatching length as calculated by the 2-cycle, Laird–Gompertz model was 3.34 mm, which agreed well

Pooled

$$SL = 3.337254e^{\left[\frac{0.071999\left(1-e^{(-0.019345\Delta_1)}\right)}{0.019345} + \frac{0.011712\left(1-e^{(-0.050839\Delta_2)}\right)}{0.050839}\right]},$$
$$\Delta_1 = MIN(Age, 31.085634)$$
$$\Delta_2 = MAX(Age - 31.085634, 0)$$

Year 1

$$SL = 3.337254e^{\left[\frac{0.074833\left(1-e^{(-0.023438\Delta_1)}\right)}{0.023438} + \frac{0.014880\left(1-e^{(-0.058754\Delta_2)}\right)}{0.058754}\right]},$$
$$\Delta_1 = MIN(Age, 31.140947)$$
$$\Delta_2 = MAX(Age - 31.140947, 0)$$

Year 2

$$SL = 3.337254e^{\left[\frac{0.073058\left(1-e^{(-0.016744\Delta_1)}\right)}{0.016744} + \frac{0.008855\left(1-e^{(-0.040660\Delta_2)}\right)}{0.040660}\right]},$$
$$\Delta_1 = MIN(Age, 31.040031)$$
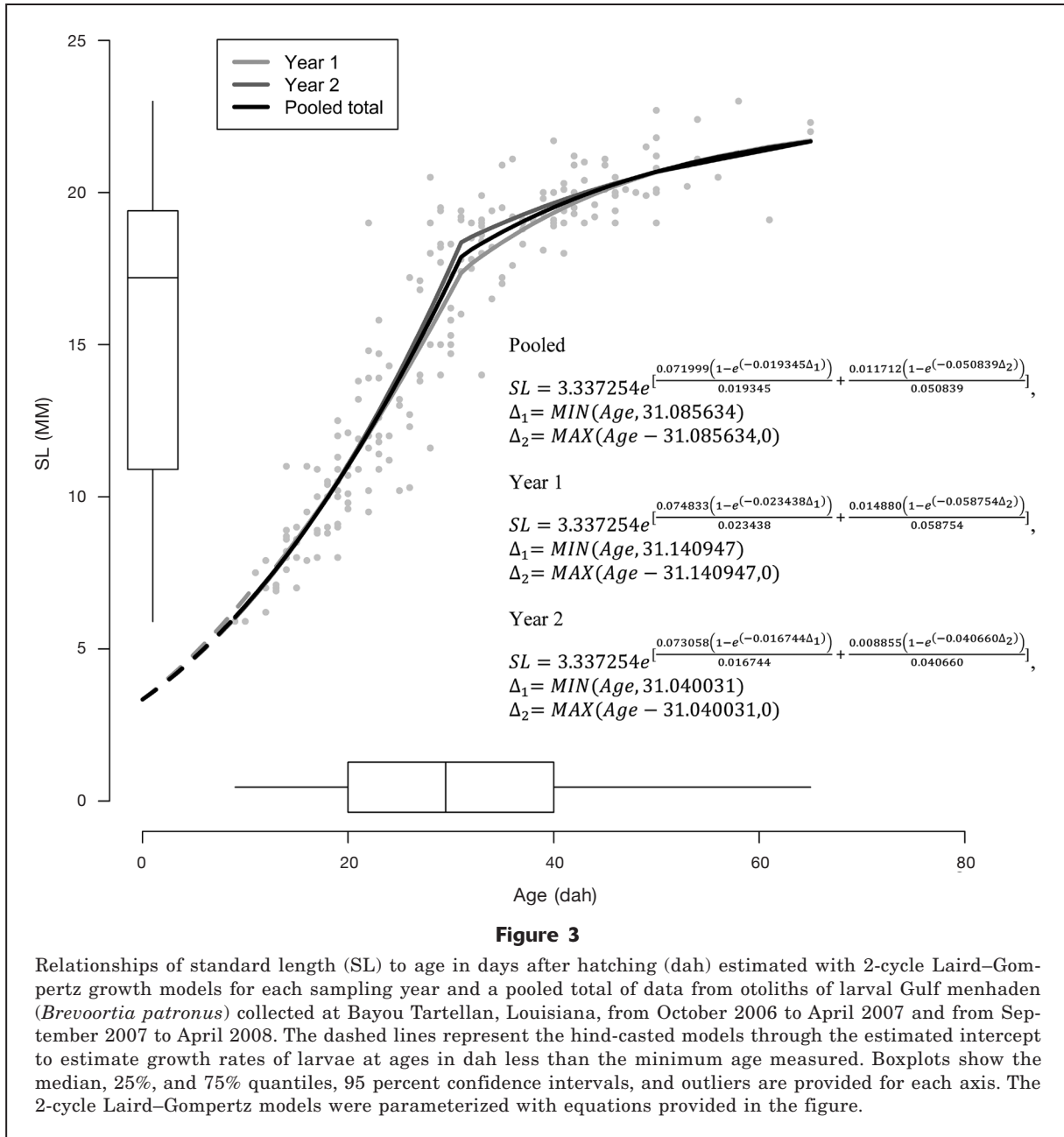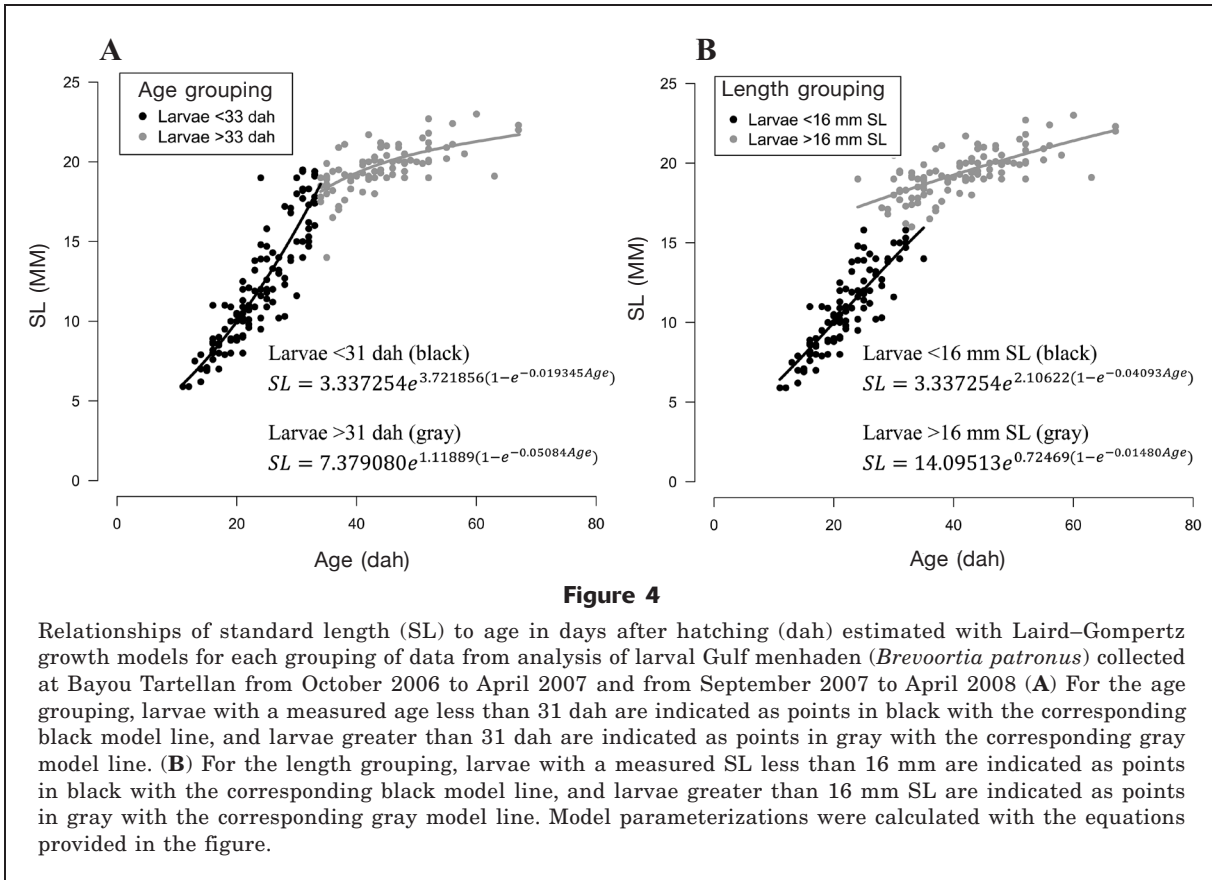$$\Delta_2 = MAX(Age - 31.040031, 0)$$

Figure 3

Relationships of standard length (SL) to age in days after hatching (dah) estimated with 2-cycle Laird–Gompertz growth models for each sampling year and a pooled total of data from otoliths of larval Gulf menhaden (*Brevoortia patronus*) collected at Bayou Tartellan, Louisiana, from October 2006 to April 2007 and from September 2007 to April 2008. The dashed lines represent the hind-casted models through the estimated intercept to estimate growth rates of larvae at ages in dah less than the minimum age measured. Boxplots show the median, 25%, and 75% quantiles, 95 percent confidence intervals, and outliers are provided for each axis. The 2-cycle Laird–Gompertz models were parameterized with equations provided in the figure.

with approximately the 3 mm total length reported elsewhere (Hettler, 1981; Warlen, 1988; Powell, 1994; Raynie and Shaw, 1994). Smaller and younger larvae were encountered earlier during the sample period (i.e., September to early October) for both years. Early September estuarine recruitment of Gulf menhaden larvae is novel for Louisiana waters (Raynie and Shaw, 1994; Carassou et al., 2012), and the smaller sizes and younger ages suggest a truncated recruitment corridor and spawning that occurs earlier than previously reported and within more coastal waters (Shaw et al., 1988). The shorter distance of the spawning ground to estuary recruitment corridor at this time of year may possibly be a result of the influences of the off-shore GOM hypoxia zone that shifts spawning aggregations into a narrow, alongshore corridor (Vaughan et al., 2007). Although there is still much debate on the role that hypoxia may play in fisheries production (Chesney and Baltz, 2001; Breitburg, 2002; Diaz and Rosenberg, 2008), such a shortened spawning-ground to estuary-recruitment corridor, may drive earlier estuarine recruitment for larval Gulf menhaden, thereby decreasing offshore mortality during larval drift (Cushing, 1974; Letcher et al., 1996).
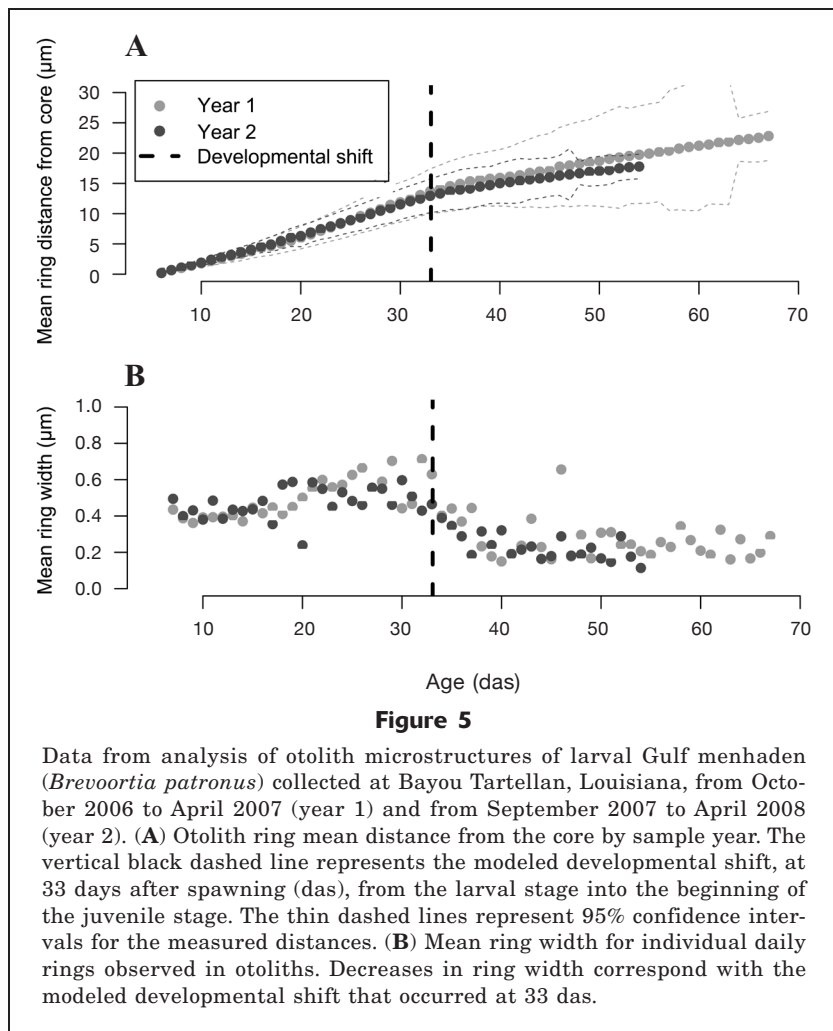
Spawning dates back calculated from ages (das) suggested movement of spawning aggregations far-

Figure 4

Relationships of standard length (SL) to age in days after hatching (dah) estimated with Laird–Gompertz growth models for each grouping of data from analysis of larval Gulf menhaden (*Brevoortia patronus*) collected at Bayou Tartellan from October 2006 to April 2007 and from September 2007 to April 2008 (**A**) For the age grouping, larvae with a measured age less than 31 dah are indicated as points in black with the corresponding black model line, and larvae greater than 31 dah are indicated as points in gray with the corresponding gray model line. (**B**) For the length grouping, larvae with a measured SL less than 16 mm are indicated as points in black with the corresponding black model line, and larvae greater than 16 mm SL are indicated as points in gray with the corresponding gray model line. Model parameterizations were calculated with the equations provided in the figure.

ther offshore as the season progressed (Whitehead, 1985; Vaughan et al., 2007). Spawning was bimodal in both years and peaked during fall in either October or November, depending on year. This peak was smaller than the second, late-winter peak, which occurred in either late January or early February for years 1 and 2, respectively. This large second spawning peak is consistent with previously reported spawning peaks that occurred in late January and February (Shaw et al., 1988; Powell 1994; Raynie and Shaw, 1994; Vaughan et al., 2000). In particular, collection of small (3–5 mm SL) and young (7–12 das) larvae in late September to early October had back-calculated spawning dates that suggested a much earlier spawning season (i.e., September) and a much shorter recruitment corridor than previously reported. Overall, the larvae of the fall spawning peak were generally smaller (mean: 14 mm SL), and younger (22 das) than the larvae that composed the winter peak (mean: 19 mm SL; age: 41 das). The fall peak, however, corresponded with a shorter recruitment corridor and transit time (i.e., approximately 3 weeks) compared with the winter peak with transport times of approximately 6 weeks. The fall transit time, therefore, is much shorter than the transport time of 4–10 weeks estimated by Shaw et al. (1988) but corresponds well with adults being distributed along the coast in nearshore waters during late summer or early

fall before moving farther offshore in October (Ahrenholz, 1991) and perhaps being somewhat constrained by the Louisiana hypoxic zone (Vaughan et al., 2007).

The greatest larval growth rate was determined to occur a few days before the beginning of the ontogenetic transformation from a selective particulate feeding to omnivorous filter feeding, and during the shift from oceanic waters through the coastal boundary zone into the estuary, but there was some variability between sampling years. The 2-cycle Laird–Gompertz model estimated a maximum growth rate for the initial larval stage of 0.72 mm/day at 33 das, which was similar to the individual age-grouped Laird–Gompertz model of 0.71 mm/day at 33 das, and both models had higher maximum growth rates than those estimated with the SL-grouped Laird–Gompertz model (0.41 mm/day). The individual Laird–Gompertz models grouped by SL showed agreement and had a mean calculated growth of 0.38 mm/day that agrees with previously reported values of 0.36 mm/day (Raynie, 1991) and 0.37 mm/day (Warlen, 1988). However, the agreement among the 2-cycle Laird–Gompertz models in our study, the individual Laird–Gompertz models grouped by age, and the results by Raynie and Shaw (1994), suggests that timing of the onset of metamorphic development is tied to age and ultimately ontogeny based on shifting prey fields (Ditty, 2002). Any differences in length at

Figure 5

Data from analysis of otolith microstructures of larval Gulf menhaden (*Brevoortia patronus*) collected at Bayou Tartellan, Louisiana, from October 2006 to April 2007 (year 1) and from September 2007 to April 2008 (year 2). (**A**) Otolith ring mean distance from the core by sample year. The vertical black dashed line represents the modeled developmental shift, at 33 days after spawning (das), from the larval stage into the beginning of the juvenile stage. The thin dashed lines represent 95% confidence intervals for the measured distances. (**B**) Mean ring width for individual daily rings observed in otoliths. Decreases in ring width correspond with the modeled developmental shift that occurred at 33 das.

the ontogenetic shift from selective particulate feeding to omnivorous filter feeding—an increase that suggests a direct relationship between the ontogenetic shift and otolith deposition. The high growth rate before the shift in feeding strategy may be the result of a cumulative experience of adjusting to food source or environmental resources, before learning new feeding skills to accommodate the ongoing development of new feeding structures (Stoecker and Govoni, 1984; Deegan, 1990; Maillet and Checkley, 1990; Lozano et al., 2012).

There was overwhelming agreement with the pooled 2-cycle Laird–Gompertz model, with the fit of the 2-cycle Laird–Gompertz models for each individual year, and with the otolith microstructure analysis, for the mean age for the shift in growth. This growth stanza is a reflection of 1) transitioning from offshore spawning grounds through the coastal boundary layer and to an estuarine water mass with differing primary productivities and 2) the onset at which the ontogenetic shift from the larval stage to the juvenile stage begins. The modeled shift in growth (33 das) coincides with the previously reported shift in growth rate at 33.6 das for Gulf menhaden in Fourleague Bay, Louisiana (Raynie and Shaw, 1994). Mean distance from the otolith core and mean ring width decreased after 33 das, which probably reflects limited feeding at this point owing to the ontogenetic shift (Deegan, 1990; Raynie, 1991; Warlen, 1992; Lozano and Houde, 2013). Transforming larvae at this age, which were between approximately 19 and 21 mm SL, may be expending more energy in the development of a feeding apparatus as they change food source for the juvenile and adult stage (Deegan, 1990; Maillet and Checkley, 1990), and in deepening their body rather than increasing length (Deegan, 1990; Raynie and Shaw, 1994).

The slower growth rates during the period when feeding structures and feeding strategy begin to change were similar across sampling years and modeling techniques. The growth rates for the pooled model (0.11 mm/day) and yearly two-cycle models (year 1, 0.12 mm/day; year 2, 0.10 mm/day) showed strong agreement with the rates for the age-grouped Laird–Gompertz models (SL grouping: 0.10 mm/day; age grouping: 0.08 mm/day). Although useful in comparisons with previous work, the age-grouped Laird–Gompertz models are less parsimonious and did not capture the ontogenetic shift in feeding strategy from a selective particulate filter feeder to an omnivorous filter feeder, except through

these ages is likely to be due to the variability of food sources or other resources that result in differences in the instantaneous larval growth rate (Warlen, 1988; Lyczkowski-Shultz et al., 1990; Warlen, 1992) during the initial larval stage, when Gulf menhaden larvae are selective particulate feeders (Stoecker and Govoni, 1984; Deegan, 1990; Lozano et al., 2012).

Differences in water temperature between sampling year 1 and 2 are correlated with the slight differences in growth rate and otolith microstructure between both years. In year 1 the highest growth rate was 0.63 mm/day and was much lower than the maximum growth rate in year 2 (0.77 mm/day), when overall warmer water temperatures likely aided increased somatic growth (Houde, 1974; Heimbuch et al., 2007). However, differences in mean ring distance from the otolith core, although small, showed the opposite trend, with slightly faster otolith ring growth during year 1. Previous research has revealed a similar decoupling between otolith growth and somatic growth (Mosegaard et al., 1988; Fey, 2006). Despite this partial decoupling, otolith microstructure for both years showed an increase in otolith ring width directly before the beginning of

interpretation. The switch of feeding from a selective particulate zooplanktivorous strategy to an omnivorous filter-feeding strategy is likely to drive the lower growth rate during this period (Deegan, 1990; Maillet and Checkley, 1990; Chen et al., 1992; Lozano et al., 2012). Moreover, the decrease in otolith ring width suggested that although daily rings were still accrued, there was limited growth during this time period. Previously reported growth rates of 0.11 mm/day (Raynie, 1991) and 0.12 mm/day (Deegan, 1990) agree with all models in our study. Despite this reduction in growth rate during transformation to the juvenile stage, larval Gulf menhaden may typically undergo another period of rapid growth after 30 mm SL, when the larvae have acquired fully developed feeding structures and are able to filter feed effectively, with growth rates as high as 0.48 mm/day (Deegan, 1990).

Acknowledgments

Literature cited

Ahrenholz, D. W.
   1991.   Population biology and life history of the North American menhadens, *Brevoortia* spp.   Mar. Fish. Rev. 53(4):3–19.
Breitburg, D.
   2002.   Effects of hypoxia, and the balance between hypoxia and enrichment, on coastal fishes and fisheries.   Estuaries 25:767–781.   Article
Campana, S. E.
   1992.   Measurement and interpretation of the microstructure of fish otoliths.   Can. Spec. Publ. Fish. Aquat. Sci. 117:59–71.
Carassou, L., F. J. Hernandez, S. P. Powers, and W. M. Graham.
   2012.   Cross-shore, seasonal, and depth-related structure of ichthyoplankton assemblages in coastal Alabama.   Trans. Am. Fish. Soc. 141:1137–1150.   Article
Chambers, R. C., and T. J. Miller.
   1995.   Evaluating fish growth by means of otolith increment analysis: special properties of individual-level longitudinal data.   *In* Recent developments in fish otolith research (D. H. Secor, J. M. Dean, and S. E. Campana, eds.), p. 155–175.   Univ. South Carolina Press, Columbia, SC.
Chesney, E. J., and D. M. Baltz.
   2001.   The effects of hypoxia on the northern Gulf of Mexico coastal ecosystem: a fisheries perspective.   *In* Coastal hypoxia: consequences for living resources and ecosystems.   Coastal and Estuarine Studies 58 (N. N. Rabalais and R. E. Turner, eds.), p. 321–354.   Am. Geophys. Union, Washington, DC.
Chen, W., J. J. Govoni, and S. M. Warlen.
   1992.   Comparison of feeding and growth of larval round herring *Etrumeus teres* and gulf menhaden *Brevoortia patronus*.   Fish. Bull. 90:183–189.
Cushing, D. H.
   1974.   The possible density-dependence of larval mortality and adult mortality in fishes.   *In* The early life history of fish: proceedings of an international symposium held at the Dunstaffnage Marine Research Laboratory of the Scottish Marine Biological Association; Oban, Scotland, 17–23 May (J. H. S. Blaxter ed.), p. 103–111.   Springer-Verlag, Berlin.
   1975.   Marine ecology and fisheries, 278 p.   Cambridge Univ. Press, Cambridge, England.
Dahlberg, M. D.
   1970.   Atlantic and Gulf of Mexico menhadens, genus *Brevoortia* (Pisces: Clupeidae).   Bull. Fla. Mus. Nat. Hist. Biol. Sci. 15:91–162.
Deegan, L. A.
   1990.   Effects of estuarine environmental conditions on population dynamics of young-of-the-year gulf menhaden.   Mar. Ecol. Prog. Ser. 68:195–205.
Deegan, L. A., and B. A. Thompson.
   1987.   Growth rate and life history events of young-of-the-year gulf menhaden as determined from otoliths.   Trans. Am. Fish. Soc. 116:663–667.   Article
Del Rio, R., S. Bargu, D. Baltz, S. Fire, G. Peterson, and Z. Wang.
   2010.   Gulf menhaden (*Brevoortia patronus*): a potential vector of domoic acid in coastal Louisiana food webs.   Harmful Algae 10:19–29.   Article
Diaz, R. J., and R. Rosenberg.
   2008.   Spreading dead zones and consequences for marine ecosystems.   Science 321: 926–929.   Article
Ditty, J. G.
   2002.   Ontogeny and intervals of development in five reef-associated species of blenny from the northern Gulf of Mexico (Teleostei: Blenniidae).   Ph.D. diss., 155 p.   Louisiana State Univ., Baton Rouge, LA.   [Available from website.]
Epifanio, C. E., and R. W. Garvine.
   2001.   Larval transport on the Atlantic continental shelf of North America: a review.   Est. Coast. Shelf Sci. 52:51–57.   Article
Fahay, M. P.
   2007.   Early stages of fishes in the western North Atlantic Ocean (Davis Strait, Southern Greenland and Flemish Cap to Cape Hatteras), vol. 2: Scorpaeniformes through Tetraodontiformes, 764 p.   Northwest Atlantic Fisheries Organization, Dartmouth, Canada.
Fey, D. P.
   2006.   The effect of temperature and somatic growth on otolith growth: the discrepancy between two clupeid species from a similar environment.   J. Fish Biol. 69:794–806.   Article
Gaemers, P. A. M.
   1976.   New concepts in the evolution of the Gadidae (Vertebrata, Pisces), based on their otoliths.   Meded. Werkgr. Tert. Kwart. Geol.13:3–32.
Geffen, A. J.
   1992.   Validation of otolith increment deposition rate.   Can. Spec. Publ. Fish. Aquat. Sci. 117:101–113.

Gillanders, B. M., K. W. Able, J. A. Brown, D. B. Eggleston, and P. F. Sheridan.
    2003.   Evidence of connectivity between juvenile and adult habitats for mobile marine fauna: an important component of nurseries.   Mar. Ecol. Prog. Ser. 247:281–295. Article

Gompertz, B.
    1825.   On the nature of the function expressive of the law of human mortality, and on a new mode of determining the value of life contingencies.   Philos. Trans. R. Soc. Lond., B 115:513–585.   Article

Guillory, V., J. Geaghan, and J. Roussel.
    1983.   Influence of environmental factors on Gulf menhaden recruitment.   Tech. Bull. 37, 32 p.   Louisiana Dep. Wildl. Fish., New Orleans, LA.

Heimbuch, D. G., E. Lorda, D. Vaughan, L. W. Barnthouse, J. Uphoff, W. Van Winkle, A. Kahnle, B. Young, J. Young, and L. Kline.
    2007.   Assessing coastwide effects of power plant entrainment and impingement on fish populations: Atlantic menhaden example.   North Am. J. Fish. Manage. 27:569–577.   Article

Hettler, W. F.
    1981.   Spawning and rearing Atlantic menhaden.   Prog. Fish-Cult. 43:80–84.   Article

Houde, E. D.
    1974.   Effects of temperature and delayed feeding on growth and survival of larvae of three species of subtropical marine fishes.   Mar. Biol. 26:271–285.   Article

Isermann, D. A., and C. T. Knight.
    2005.   A computer program for age–length keys incorporating age assignment to individual fish.   North Am. J. Fish. Manage. 25:1153–1160.   Article

Kupchik, M. J., and R. F. Shaw.
    2016.   Age, growth, and recruitment of larval and early juvenile Atlantic croaker (*Micropogonias undulatus*), determined from analysis of otolith microstructure.   Fish. Bull. 114:18–33.   Article

Laird, A. K., S. A. Tyler, and A. D. Barton.
    1965.   Dynamics of normal growth.   Growth 29:233–248.

Letcher, B. H., J. A. Rice, L. B. Crowder, and K. A. Rose.
    1996.   Variability in survival of larval fish: disentangling components with a generalized individual-based model.   Can. J. Fish. Aquat. Sci. 53:787–801.   Article

Lewis, R. M., and C. M. Roithmayr.
    1981.   Spawning and sexual maturity of Gulf menhaden, *Brevoortia patronus*.   Fish. Bull. 78:947–951.

Lombarte, A., and B. Morales-Nin.
    1995.   Morphology and ultrastructure of saccular otoliths from five species of the genus *Coelorincus* (Gadiformes: Macrouridae) from the southeast Atlantic.   J. Morphol. 225:179–192.   Article

Lozano, C., and E. D. Houde.
    2013.   Factors contributing to variability in larval ingress of Atlantic menhaden, *Brevoortia tyrannus*.   Est. Coast. Shelf Sci. 118:1–10.   Article

Lozano, C., E. D. Houde, R. L. Wingate, and D. H. Secor.
    2012.   Age, growth and hatch dates of ingressing larvae and surviving juveniles of Atlantic menhaden *Brevoortia tyrannus*.   J. Fish Biol. 81:1665–1685.   Article

Lyczkowski-Shultz, J., D. L. Ruple, S. L. Richardson, and J. H. Cowan Jr.
    1990.   Distribution of fish larvae relative to time and tide in a Gulf of Mexico barrier island pass.   Bull. Mar. Sci. 46:563–577.

Maillet, G. L., and D. M. Checkley Jr.
    1990.   Effects of starvation on the frequency of formation and width of growth increments in sagittae of laboratory-reared Atlantic menhaden Brevoortia tyrannus larvae.   Fish. Bull. 88:155–165.
    1991.   Storm-related variation in the growth rate of otoliths of larval Atlantic menhaden *Brevoortia tyrannus*: a time series analysis of biological and physical variables and implications for larva growth and mortality.   Mar. Ecol. Prog. Ser. 79:1–16.

Marotz, B. L., W. H. Herke, and B. D. Rogers.
    1990.   Movement of Gulf menhaden through three marshland routes in southwestern Louisiana.   North Am. J. Fish. Manage. 10:408–417.   Article

McCrea-Strub, A., K. Kleisner, U. R. Sumaila, W. Swartz, R. Watson, D. Zeller, and D. Pauly.
    2011.   Potential impact of the *Deepwater Horizon* oil spill on commercial fisheries in the Gulf of Mexico.   Fisheries 36:332–336.   Article

Morales-Nin, B., A. Lombarte, and B. Japón.
    1998.   Approaches to otolith age determination: image signal treatment and age attribution.   Sci. Mar. 62:247–256.

Mosegaard, H., H. Svedäng, and K. Taberman.
    1988.   Uncoupling of somatic and otolith growth rates in Arctic char (*Salvelinus alpinus*) as an effect of differences in temperature response.   Can. J. Fish. Aquat. Sci. 45:1514–1524.   Article

Nelson, W. R., and D. W. Ahrenholz.
    1986.   Population and fishery characteristics of gulf menhaden, *Brevoortia patronus*.   Fish. Bull. 84:311–325.

Nelson, J., R. Wilson, F. Coleman, C. Koenig, D. DeVries, C. Gardner, and J. Chanton.
    2012.   Flux by fin: fish-mediated carbon and nutrient flux in the northeastern Gulf of Mexico.   Mar. Biol. 159:365–372.   Article

Nolf, D.
    1985.   Otolithi piscium.   *In* Handbook of paleoichthyology, vol. 10 (M. P. Schultze, ed.), 145 p.   Gustav Fisher Verlag, Stugart, Germany.

Powell, A. B.
    1994.   Life history traits of two allopatric clupeids, Atlantic menhaden and gulf menhaden, and the effects of harvesting on these traits.   North Am. J. Fish. Manage. 14:53–64.   Article

Pritchard, E. S. (ed.).
    2005.   Fisheries of the United States 2004. Current Fishery Statistics No. 2004, 109 p.   Natl. Mar. Fish. Serv., Silver Spring, MD.   [Available from website.]

R Core Team.
    2014.   R: a language and environment for statistical computing.   R Foundation for Statistical Computing, Vienna, Austria.   [Available from website, accessed August 2014.]

Ralston, S., and H. Williams.
    1989.   Numerical integration of daily growth increments: an efficient means of aging tropical fishes for stock assessment.   Fish. Bull. 87:1–16.

Raynie, R. C.
    1991.   Study of the spatial and temporal ichthyoplankton abundance along a recruitment corridor from offshore to estuarine nursery.   M.S. thesis, 115 p.   Louisiana State Univ., Baton Rouge, LA.

Raynie, R. C., and R. F. Shaw.
　　1994.　Ichthyoplankton abundance along a recruitment corridor from offshore spawning to estuarine nursery ground.　Est. Coast. Shelf Sci. 39:421–450.　Article

Richards, W. J. (ed.).
　　2005.　Early stages of Atlantic fishes: an identification guide for the western central North Atlantic, vols. I and II, 2640 p.　CRC Press, Boca Raton, FL.

Schmidt, W.
　　1969.　The otoliths as a mean for differentiation between species of very similar appearance.　*In* Proceedings of the symposium on the oceanography and fisheries of the tropical Atlantic; Abidjan, Côte d'Ivoire, 20–28 October 1966, p. 393–396.　UNESCO, Paris.

Shanks, A. L., and G. L. Eckert.
　　2005.　Population persistence of California Current fishes and benthic crustaceans: a marine drift paradox.　Ecol. Monogr. 75:505–524.　Article

Shaw, R. F., W. J. Wiseman Jr., R. E. Turner, L. J. Rouse Jr., R. E . Condrey, and F. J. Kelly Jr.
　　1985.　Transport of larval gulf menhaden *Brevoortia patronus* in continental shelf waters of western Louisiana: a hypothesis.　Trans. Am. Fish. Soc. 114:452–460.　Article

Shaw, R. F., B. D. Rogers, J. Cowan, and W. H. Herke.
　　1988.　Ocean-estuary coupling of ichthyoplankton and nekton in the northern Gulf of Mexico.　*In* Larval fish and shellfish transport through inlets (M. P. Weinstein, ed.), p. 77–89.　Am. Fish. Soc., Bethesda, MD.

Simonsen, K. A., and J. H. Cowan.
　　2013.　Effects of an inshore artificial reef on the trophic dynamics of three species of estuarine fish.　Bull. Mar. Sci. 89:657–676.　Article

Stoecker, D. K., and J. J. Govoni.
　　1984.　Food selection by young larval gulf menhaden (*Brevoortia patronus*).　Mar. Biol. 80:299–306.　Article

Suttkus, R. D.
　　1956.　Early life history of the gulf menhaden, *Brevoortia patronus*, in Louisiana.　Trans. North Am. Wildl. Conf. 21:390–407.

Vaughan, D. S., J. W. Smith, and M. H. Prager.
　　2000.　Population characteristics of Gulf menhaden, *Brevoortia patronus*.　NOAA Tech. Rep. NMFS 149, 19 p.

Vaughan, D. S., K. W. Shertzer, and J. W. Smith.
　　2007.　Gulf menhaden (*Brevoortia patronus*) in the U.S. Gulf of Mexico: fishery characteristics and biological reference points for management.　Fish. Res. 83:263–275.　Article

Warlen, S. M.
　　1988.　Age and growth of larval gulf menhaden, *Brevoortia patronus*, in the northern Gulf of Mexico.　Fish. Bull. 86:77–90.
　　1992.　Age, growth, and size distribution of larval Atlantic menhaden off North Carolina.　Trans. Am. Fish. Soc. 121:588–598.　Article

Whitehead, P. J. P.
　　1985.　FAO species catalogue. Clupeoid fishes of the world: an annotated and illustrated catalogue of the herrings, sardines, pilchards, sprats, shads, anchovies and wolf-herrings. Part 1—Chriocentridae, Clupeidae and Pristigasteridae.　FAO Fish. Synop. 125, vol. 7, 303 p.　FAO, Rome.

Zweifel, J. R., and R. Lasker.
　　1976.　Prehatch and posthatch growth of fishes—a general model.　Fish. Bull. 74:609–621.